

Received February 28, 2021, accepted March 22, 2021, date of publication March 29, 2021, date of current version April 7, 2021.

Digital Object Identifier 10.1109/ACCESS.2021.3069282

Investigation of the Effect of Sonication Time on Dispersion Stability, Dielectric Properties, and Heat Transfer of Graphene Based Green Nanofluids

RIZWAN A. FARADE¹, NOOR IZZRI ABDUL WAHAB¹, (Senior Member, IEEE),
DIAA-ELDIN A. MANSOUR², (Senior Member, IEEE),
NORHAFIZ B. AZIS¹, (Senior Member, IEEE),
JASRONITA BT. JASNI¹, (Senior Member, IEEE),
VEERAPANDIYAN VEERASAMY¹, (Graduate Student Member, IEEE),
MARIAMMAL THIRUMENI³,
ANDREW XAVIER RAJ IRUDAYARAJ¹, (Graduate Student Member, IEEE),
AND AVINASH SRIKANTA MURTHY¹

¹Department of Electrical and Electronics Engineering, Faculty of Engineering, University Putra Malaysia, Serdang 43400, Malaysia

²Department of Electrical Power and Machines Engineering, Faculty of Engineering, Tanta University, Tanta 31511, Egypt

³Department of Electrical and Electronics Engineering, Rajalakshmi Engineering College, Chennai 602105, India

Corresponding authors: Rizwan A. Farade (rizwan.projects@gmail.com) and Noor Izzri Abdul Wahab (izzri@upm.edu.my)

This work was supported in part by the University Putra Malaysia under Grant GPB 9630000.

ABSTRACT Natural ester oils are the current target of many industries and electrical utilities as electrically insulating fluids to replace the conventional mineral oils. However, as previously investigated, most natural ester oils are based on edible products, causing a negative impact on the food crisis. Accordingly, nonedible green nanofluids based on cottonseed oil have been targeted in the present study. Additive graphene nanoparticles (0.0015 wt%, 0.003 wt%, 0.006 wt%, and 0.01 wt%) along with surfactant sodium dodecylbenzene sulfonate (SDBS) were used (1:1) due to their promising impact on dielectric and thermal properties. Experimental methods introduced were including characterization of graphene and preparation of dielectric nanofluids (DNFs). The main concern for any nanofluid to be usable in transformer applications is its long-term stability. The effect of various ultrasonication periods (10, 20, 30 and 60-minute) on short-term stability of nanofluids was preliminary investigated by visual inspection, highest short-term stability was obtained at 30-min and 60-min. Considering short-term stability results, the two most stable samples were investigated and compared for long-term stability through ultraviolet-visible (UV-Vis) spectroscopy to find the suitable ultrasonication time. In addition, dielectric and thermal properties of these samples were investigated and compared. Physical mechanisms were discussed for the obtained enhancements considering the effect of ultrasonication period on the number of dispersed nanoparticle sheets per unit volume and the corresponding effect on dielectric and thermal properties.

INDEX TERMS Graphene, ultrasonication, stability of nanofluids, dielectric properties, thermal conductivity.

NOMENCLATURE

BDV Breakdown voltage
CSO Cottonseed oil

DBF Dielectric base fluid
DNF Dielectric nanofluid
EDL Electrical double layer
Enh. Enhancement
Expt. Experiment
RTP Room temperature and pressure

The associate editor coordinating the review of this manuscript and approving it for publication was Abhishek K. Jha¹.

| | |
|--------|------------------------------------|
| SAED | Selected-area electron diffraction |
| SDBS | Sodium dodecyl benzene sulfonate |
| SDS | Sodium dodecyl sulfate |
| Std. | Standard |
| TBHQ | Tertiary butylhydroquinone |
| UV-Vis | Ultraviolet–visible |
| wt% | Weight percentage |

I. INTRODUCTION

Dielectric nanofluids (DNFs) have gained a great interest for the application with power transformers. Usually these types of fluids are based on mineral oils. But, due to the environmental concerns, safety issues, and running out of fossil fuel, ester oils have been proposed as an alternative for mineral oils [1]–[4]. Ester oils can be natural ester oils or synthetic ones. Natural ester oils have the advantages of better biodegradability and higher flash and fire points compared to mineral oils. In addition, natural ester oils proved to decrease the transformer aging and its loss of life [5], [6]. The only drawback of natural ester oils is their high viscosity which negatively impacts the oil flow within the transformer and the subsequent heat transfer to the surrounding.

Using natural ester oils as base fluids for dielectric nanofluids has been extensively investigated in recent years, where nanofluid concept could enhance the dielectric and thermal properties of such oils. In this regard, different types of nanoparticles have been used [7]–[9].

For the enhancement of dielectric properties, usually metal oxides are used. In [10], three different types of nanoparticles were used with natural ester oil, Fe_3O_4 , SiO_2 and Al_2O_3 . The enhancement in AC breakdown voltage (BDV) didn't exceed 7% and was obtained with Fe_3O_4 at 0.4 g/L concentration and with Al_2O_3 at 0.05 g/L concentration. Similarly, Fe_3O_4 and Al_2O_3 nanoparticles exhibited higher enhancements compared to BN nanoparticles [11]. In [12], TiO_2 and ZnO nanoparticles were also used with natural ester. The percentage enhancement in BDV with TiO_2 nanoparticles attained about 33% at a concentration of 0.04 wt%, while the percentage enhancement with ZnO nanoparticles attained about 26% at a concentration of 0.04 wt%. When compared TiO_2 nanoparticles with Fe_2O_3 ones in [13], TiO_2 nanoparticles could enhance the BDV up to about 67%, while the enhancement was limited to 20% with Fe_2O_3 nanoparticles. Also, TiO_2 nanoparticles at 0.02 vol% enhanced the BDV up to 22% for EnvirotempTMFR3 natural ester oil from Cargill Industrial Specialties–Minneapolis, MN, USA [14]. In spite of TiO_2 nanoparticles proved several enhancements in dielectric properties with different natural ester oils, they failed to enhance thermal conductivity of these oils [15].

For the enhancement in thermal properties, only special types could enhance the thermal properties of natural ester oils. In [16], using $\text{CaCu}_3\text{Ti}_4\text{O}_{12}$ nanoparticles at a concentration of 0.05 vol% could enhance the thermal conductivity for synthetic ester about 10% and 9% at room temperature and 80 °C, respectively. Molybdenum disulfide (MoS_2) and h-BN

nanoparticles were also used either as individual type or as hybrid together to enhance the thermal conductivity for several commercially-type natural esters [17]. Hybrid nanostructures of h-BN/ MoS_2 exhibited the highest enhancement in thermal conductivity. When using Midel 7131 from M&I Materials-Manchester, UK, the hybrid nanostructures exhibited a maximum enhancement of 32% at 0.25 wt% and 323 K, while MoS_2 and h-BN nanoparticles exhibited enhancements of 26.5% and 24.2%, respectively, at the same weight fraction and temperature.

Most of previous studies on natural ester oils and their nanofluids were based on edible products. Considering the large consumption of insulating fluids in power transformers, using edible oils for this purpose will negatively impact the food crisis. Few studies have investigated the usage of nonedible oils as electrically insulating fluids [18]–[20]. In [18], *Jatropha curcas* methyl ester oil and its mixtures with mineral oil were investigated for BDV under AC and DC voltage application. In [19] cottonseed oil (CSO) based nanofluids were developed using h-BN nanoparticles resulting in enhancements in both thermal and dielectric properties. Also, CSO based nanofluids were developed in [20], but with using graphene oxide nanoparticles and SDS as surfactant. When using graphene oxide nanoparticles, the enhancement in thermal conductivity of CSO based nanofluids was higher than that obtained when using h-BN nanoparticles, however, the enhancement in AC BDV was limited.

To get the beneficial properties from DNFs, a stable DNF is desired, in which nanoparticles suspended into the fluid for a long-term. This can be achieved through homogeneous dispersion of nanoparticles when steric repulsion force dominates Van der Waals attraction force [21]. Few researchers investigated stability of DNFs for use in transformers [22]–[26]. Most works concluded that a low filler level leads better stability than higher filler level [27], due to decreased probability of collision between nanoparticles to form aggregates. It is also evident from these studies that all authors adopted visual inspection evaluation method to determine the dispersion stability. Visual inspection method is a qualitative method and is less effective, therefore quantitative UV-Vis method was adopted for current investigation. The surfactant shields nanoparticles, which prevents the forming of bonds with other nanoparticles by steric interactions. Some studies report that addition of significant quantities of surfactant can shorten the dispersal time and weaken the dielectric properties of DNFs [28], [29].

This study aims to develop CSO based DNFs with long-term stability using a combination of graphene and SDBS with optimized ultrasonication period. First, experimental methods were introduced including characterization of graphene, preparation of DNFs and investigation of stability, dielectric properties, and thermal properties. Different ultrasonication periods of 10, 20, 30 and 60-minute were considered and DNFs were inspected visually after two weeks for short-term stability. Based on short-term stability results, unlike previously published works two

TABLE 1. Data collection instrumentation.

| Sr. No | Instrument / Expt. setup / Std. | Purpose / Accuracy | Operating condition |
|--------|---|--|---|
| 1. | Scanning Electron Microscope (SEM) Model: JSM-IT 500 InTouchScope™, JEOL Ltd., Tokyo, Japan | Morphological visualization of graphene particles | Acceleration voltage: 20 kV |
| 2. | Transmission Electron Microscope (TEM) Model: JEM 2100 PLUS, JEOL Ltd., Tokyo, Japan | Size analysis of graphene particles | High voltage: 200 kV |
| 3. | Energy-Dispersive X-Ray Spectroscopy (EDX) Model: JSM-IT 500 InTouchScope™, JEOL Ltd., Tokyo, Japan | Determination of specific elements in graphene particles | Acceleration voltage: 20 kV |
| 4. | Powder X-ray diffraction (XRD) Model: SmartLab SE, Rigaku Corporation, Tokyo, Japan | Phase purity identification of graphene particles | Cu K β radiation, 2 Θ =5-90° |
| 5. | Probe Sonicator Model: PKS-250FM, Anamatrix Instrument Technologies Private Limited, Bangalore, India | Preparation of DNFs | Power 70% Pulse 40% |
| 6. | Ultraviolet spectrometer Model: UV-1800, Shimadzu Corporation, Kyoto, Japan | Stability analysis | wavelength of 190 and 1100 nm |
| 7. | Breakdown voltage test kit Supplier: High Pot Engineers, Bangaluru, India. Test specifications: IEC 156. | AC breakdown voltages of the prepared DNFs | RTP Results: 10 breakdowns |
| 8. | Automatic relative permittivity, tan δ and resistivity test set. Model: ADTR 2K Plus, ELTEL Industries, Bangaluru, India. Standard: IEC-60247 | Relative permittivity (Accuracy: $\pm 0.1\%$), tan δ (Accuracy: $\pm 1\%$) and resistivity (Accuracy: 2-5%) measurements of DNFs | 45°C, 60°C, 75°C and 90°C AC measurements: 500 V, 50Hz DC measurements: 500 V Results: 3 times / sample |
| 9. | Thermal properties analyzer Model: KD2 Pro, Decagon Devices, Inc., Pullman, Washington, USA Standard: IEEE 442-1981 and ASTM D5334 | Thermal conductivity (Accuracy: $\pm 5\%$) measurement of DNFs | 35°C, 45°C, 55°C and 65°C Results: 3 times / sample |
| 10. | Thermal response test set Model: Custom-built as per the requirement [19]. | Confirm superior thermal conductivity of DNFs | Heating time-26 min Cooling time-26 min |

ultrasonication periods were used for preparing graphene DNFs (0.0015 wt%, 0.003 wt%, 0.006 wt%, and 0.01 wt%) for long-term stability evaluation through UV-Vis. For same two most stable ultrasonicated DNFs, dielectric and thermal properties were investigated and compared at varying temperatures (except AC BDV measured at RTP). Finally, the governing mechanisms behind the obtained results were discussed.

II. EXPERIMENTAL METHODS

A. INSTRUMENTATION FOR DATA COLLECTION

There are various experimental phases adopted in the current research. These include characterization of graphene, preparation of DNFs and investigation of dielectric and thermal properties for dielectric base fluid (DBF) and DNFs.

Table 1 summarizes the instruments used during various experimental phases, the testing conditions, and the standards followed for data collection. The table also describes in detail the purpose and accuracy of each instrument.

For AC breakdown voltage, it was measured following the IEC 156 standard, in which the electrodes are double spheres, the gap is 2.5 mm, and the rate of voltage rising is 2 kV/s. For dielectric properties, the applied voltage was set at 500 V and 50 Hz for relative permittivity and tan δ measurements and at 500 V DC for resistivity measurements. After this setting, the test cell was filled with DNFs and a test procedure was programmed to automatically set the temperatures at 45°C, 60°C, 75°C, and 90°C in ascending order. Once the test is started, the heating process is turned on till the first fixed temperature is achieved, and then the heater is cut off

automatically and measurements are made. This process is repeated for the next set values until the final temperature is reached.

For thermal conductivity, it was tested using the KD2 Pro thermal property analyzer. It utilizes a single needle sensor of 6 cm long to determine the thermal conductivity of the liquids by means of a transient hot wire technique. The water bath is used to maintain a steady temperature with 0.1 °C accuracy. The sensor is calibrated by evaluating the thermal conductivity of glycerin. Three measurements were taken within 15 minutes of the time interval between each measurement and the average value was taken. The temperature of DNFs is set in the range between 35 and 65 °C.

B. MATERIALS

Research grade multi layered graphene (UGRAY™) was obtained from United Nanotech Innovations Pvt. Ltd., India. According to the supplier technical data sheet, this multilayered graphene are of 3 to 6 sheet layer aggregates, 5-10 microns lateral dimension, 3-6 nm thickness, and 3000 W/m.K thermal conductivity. Surfactant SDBS was purchased from Sigma-Aldrich, India. Synthetic antioxidant TBHQ was supplied from Sigma-Aldrich, India. Cottonseed oil is used as DBF for the present implementation. Cottonseed oil was provided by M/s S S Odunavar Industries, India.

C. DIELECTRIC NANOFUID PREPARATION

CSO is used for the current implementation. It is vegetable oil has the main features of green oil such as non-toxicity, biodegradability and environmentally friendly. The vegetable oil with the addition of antioxidant (TBHQ) has much greater chemical stability and higher potential for antioxidant capacity. The introduction of TBHQ suppresses the decomposition of vegetable oils at elevated temperatures. Preparation of CSO DBF is already presented in our previous publication [19]. The CSO was added with 0.02% of TBHQ, and then after, the solution was stirred by magnetic stirrer at 80 °C for 1.5 hour. The water and gas contaminants have been removed from the oil through vacuum processing. Finally, the 0.0 wt% CSO (CSO DBF) became ready for the current implementation.

DNFs were prepared by liquid-phase exfoliation of graphene. DNF were prepared using the two-step process, considering its benefits. The calculated quantity of graphene was introduced to the CSO DBF and stirred by magnetic stirrer at 75 °C for 15 minutes. The dispersion stability was obtained using a probe-type ultrasonic homogenizer with an adjusted power setting of 70%, pulse setting of 40% to avoid any overheating for the samples. Considering that the power of the ultrasonic homogenizer is 250 W, this power setting will deliver 4.2 kJ of energy during each minute of sonication period. Graphene is considered a special amphiphile that have negatively charged hydrophilic edges and hydrophobic basal plane [30]. Accordingly, both cationic and anionic surfactants can interact with graphene. For cationic surfactant, the opposite charging between surfactant and graphene

is responsible for interaction between them. For anionic surfactant, similar to SDBS in our study, SDBS molecules are interacted with graphene through π - π and hydrophobic interactions [31]. So, choosing the proper surfactant in this study was based on the superior performance of graphene modified with SDBS compared to other surfactant types [31], [32]. In this case, steric stabilization is the governing mechanism by which adsorbed surfactants create intense repulsion between nanoparticles [33]. SDBS was used as a surfactant in each sample, the ratio of graphene and SDBS selected for the current implementation was 1:1. This ratio proved better stability compared to others [32]. Two separate sample groups of DNFs at each graphene weight percentage (Viz., 0.0015 wt%, 0.003 wt%, 0.006 wt%, and 0.01 wt%) were prepared with ultrasonication treatment periods 30-minute and 60-minute. Visual images of DNFs (Viz., 0.0015 wt%, 0.003 wt%, 0.006 wt%, and 0.01 wt%) with 30 and 60 minute sonication period are included in the Fig. 1.

III. GRAPHENE CHARACTERIZATION

This phase of investigation provides detailed characterization of graphene particles used for the current investigation. Graphene particles were characterized by Electron microscopy analysis, EDX, and powder XRD.

A. ELECTRON MICROSCOPY ANALYSIS OF GRAPHENE PARTICLES

Graphene SEM samples have been prepared on carbon tape bonded to a stub of aluminum. A tiny graphene sample was taken and then sprinkle over the carbon tape and the loose particles were removed after the particles stick to the carbon tape. Then, this stub was attached to the holder and placed for SEM analysis in the sample chamber. Fig. 2(a) and (b) display SEM images at 2700X and 14000X magnification levels, respectively. The morphology shows that the stacks of the few layers are loosely oriented and look like smooth silky clothes. During the preparation of TEM samples, graphene particles are dispersed in ethanol. A drop of prepared sample was put on the copper grid and was vacuum dried followed by TEM imagery. Fig. 2(c) and (d) refers to the images of graphene captured through TEM at 15000X and 30000X magnification levels, respectively. It is evident from Fig. 2(c) and (d) that the graphene sheets contain some darker areas related to the stacking of certain layers of graphene. Fig. 2(e) shows SAED pattern of graphene, showing six-fold symmetry. Fig. 2(f) shows the edge area of the graphene, indicating sheet consists of a few stacked atomic layers.

B. EDX AND XRD ANALYSIS OF GRAPHENE PARTICLES

Fig. 3(a) shows the EDX spectra of graphene, it had a carbon content of 99.79 atom% and 99.43 mass%, while the other element remains at a very low atom% and mass%. The graphene nanosheet's XRD pattern is shown in Fig. 3(b). It demonstrates that there are two distinctive peaks around $2\theta = 27^\circ$ and 54° , suggesting the material molecular structure of carbon and internal carbon atoms [34].

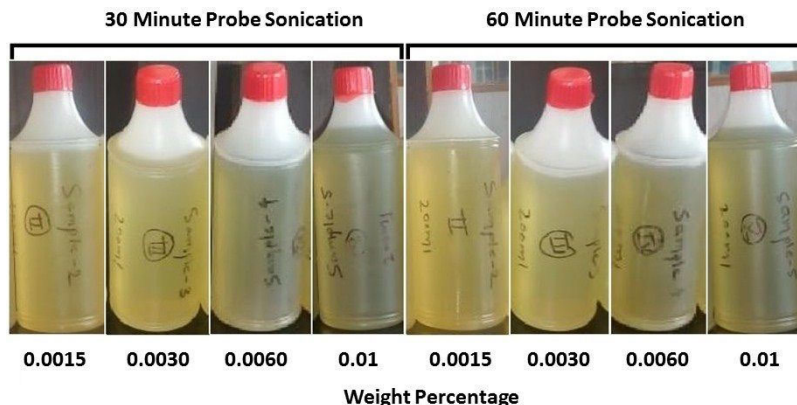


FIGURE 1. Visual Images of 30 and 60 minute sonication period dielectric nanofluid samples at varying weight percentage.

IV. EFFECTS OF ULTRASONICATION ON MULTILAYERED GRAPHENE

Graphene is composed of hexagonally arranged carbon atoms that are covalently bonded. Each sheet of graphene composes of a single-layered carbon plane. In multilayered graphene these carbon sheets are layered on top of each other, where Van der Waals weak force binds the adjacent layers together. Fig. 4(a) shows two layered graphene with covalent and Van der Waals bonds. As discussed earlier, two separate sample groups of DNF at each weight percentage (Viz., 0.0015 wt%, 0.003 wt%, 0.006 wt%, and 0.01 wt%) were prepared with ultrasonication treatment periods 30-minute and 60-minute using a probe-type ultrasonic homogenizer. Ultrasonication has a great impact on the breaking down of large nanoparticle clusters into smaller clusters along with breaking of Van der Waals bonds between layers and exfoliating graphene sheets. Once this occurs, the chains of SDBS surfactant are grafted on the surface of graphene sheets and prevent their re-accumulation [35]. Fig. 4(b) shows same two layered graphene after ultrasonication, with no Van der Waals bonds between layers.

Fig. 4(c) shows multilayered graphene stack in DNF with no ultrasonication treatment, followed by same multilayered graphene stack in DNF at lower and higher ultrasonication periods. From Fig. 4(c), it is evident that higher time of ultrasonication leads to a detachment of more graphene sheets from graphene stack by losing Van der Waals force. This will break up large nanoparticle clusters, thereby preventing particle agglomeration and sedimentation [36]. Based on this concept, it can be concluded that the higher ultrasonication period, the more homogeneous dispersion of nanoparticles in DNFs. The more the homogeneous dispersion of nanoparticles, the higher their suspension stability [37].

V. PROLONGED STABILITY OF NANOFLUIDS AT LOW AND HIGH ULTRASONICATION PERIODS

Nanoparticles are often suspended in the base fluids under the control of gravity as well as particle–fluid and particle–particle interactions. Determining the optimal ultrasonication time and power of the probe type ultrasonicator is one of the

most critical issues towards achieving the optimum dispersion stability, dielectric properties and thermal properties of DNF. Power setting of 70% and pulse setting of 40% were adopted to avoid possible overheating of DNF. Regarding ultrasonication time, using long ultrasonication times will break the clusters of nanosheets, but extreme long ultrasonication times have a negative impact on the stability and properties of obtained nanofluids [38]. Regarding dielectric nanofluids, ultrasonication times above 60 min can cause overheating with a decrement in dielectric properties. Also, previous results on nanofluids indicated that the improvement in nanofluid properties is significant only in the first 45 minutes of sonication [39]. For these reasons, as a first trial, small quantities of DNFs were prepared using four different ultrasonication times of 10, 20, 30 and 60-minute. The prepared samples were kept stationary for a period of 2 weeks and thus were examined by visual inspection. It was found that the samples prepared with the ultrasonication time of 30-minute and 60-minute are more stable than others. Thus, desired quantity of DNFs were prepared with the ultrasonication time of 30-minute and 60-minute at the required filler levels (Viz., 0.0015 wt%, 0.003 wt%, 0.006 wt%, and 0.01 wt%). Furthermore, stability of these samples was quantitatively evaluated using UV-Vis spectroscopy.

According to Beer–Lambert law, the light absorption of a solution is directly proportionate to the volume of the absorbing species in the solution. In the prepared DNFs the absorbing species are the dispersed graphene particles. Thus, for a fixed path length of sample under UV–Vis spectroscopy, the absorbance of DNFs increases with the increase in the weight percentage of graphene. Table 2 shows the peak absorbance of 30-minute and 60-minute ultrasonicated DNFs in arbitrary units (a.u.) measured after the preparation on day 1, 15, 30, 45, 60, 75, and 90. The wavelength corresponding to peak absorbance was located around 275 nm. From these results, it is evident that for the same timespan and ultrasonication time the absorbance of DNFs increases with the increase in the weight percentage of graphene. On the other hand, at fixed weight percentage (Viz., 0.0015 wt%, 0.003 wt%, 0.006 wt%, and 0.01 wt%) the absorbance of

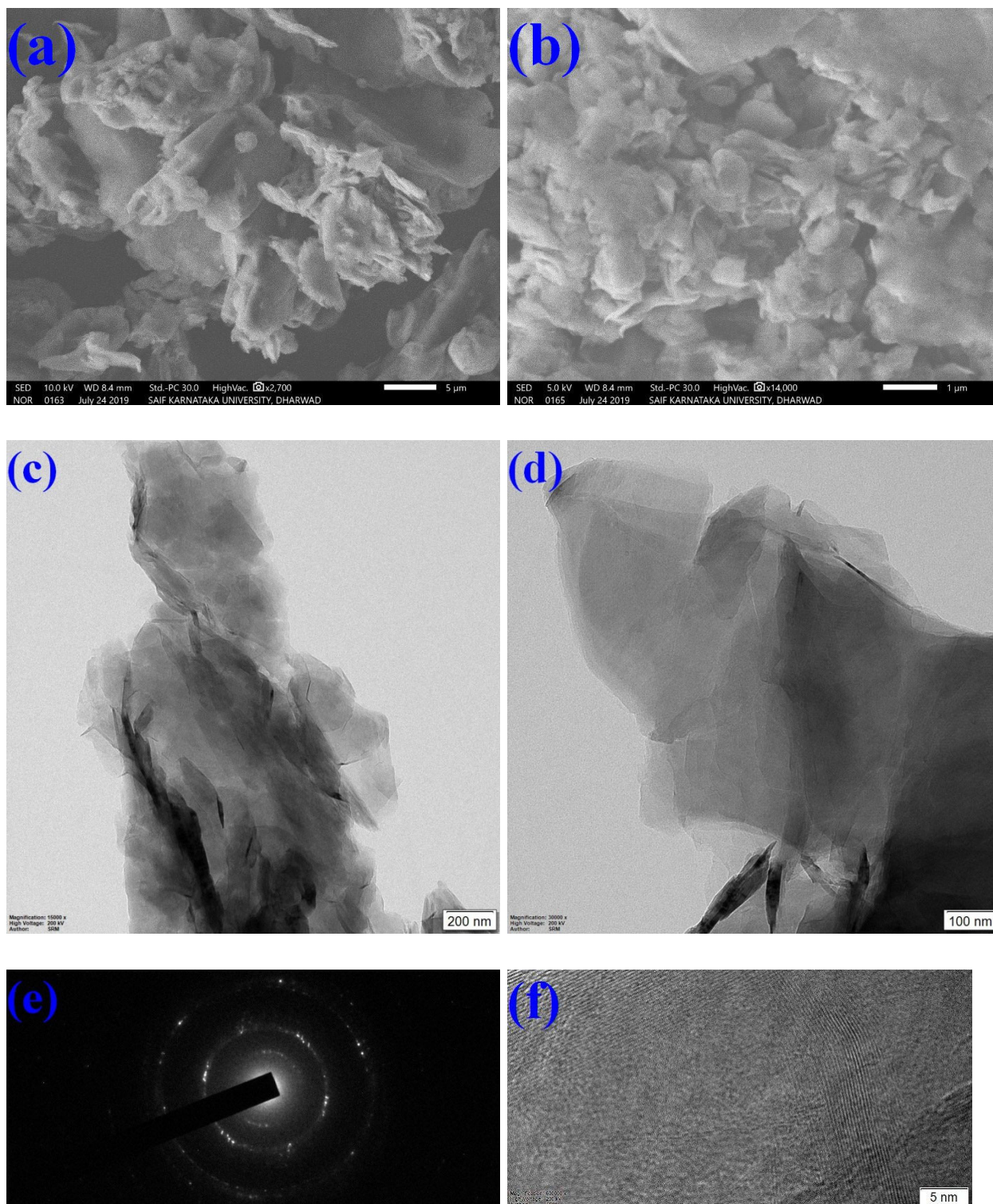


FIGURE 2. Electron microscopy analyses: Scanning Electron Microscopy (SEM) at magnification levels: a) 2700X, and b) 14000X; Transmission Electron Microscopy (TEM) at magnification levels: c) 15000X, and d) 30000X; e) Selected-area electron diffraction (SAED) pattern showing six fold symmetry; and f) TEM image illustrating the edges of the few-layered graphene.

60-minute ultrasonicated DNF is higher compared to that of 30-minute ultrasonicated DNF. On day 1, the highest absorbance of 30-minute ultrasonicated DNFs was found to be 0.903 a.u. and that of 60-minute ultrasonicated DNFs was found to be 1.161 a.u. at 0.01 wt%.

A slight portion of dispersed particles may settle down from the fluid with the prolonged time, which can result in a reduced absorption in the same DNFs at the same fixed path length. This is evident in Table 2, where at fixed weight percentage (Viz., 0.0015 wt%, 0.003 wt%, 0.006 wt%, and

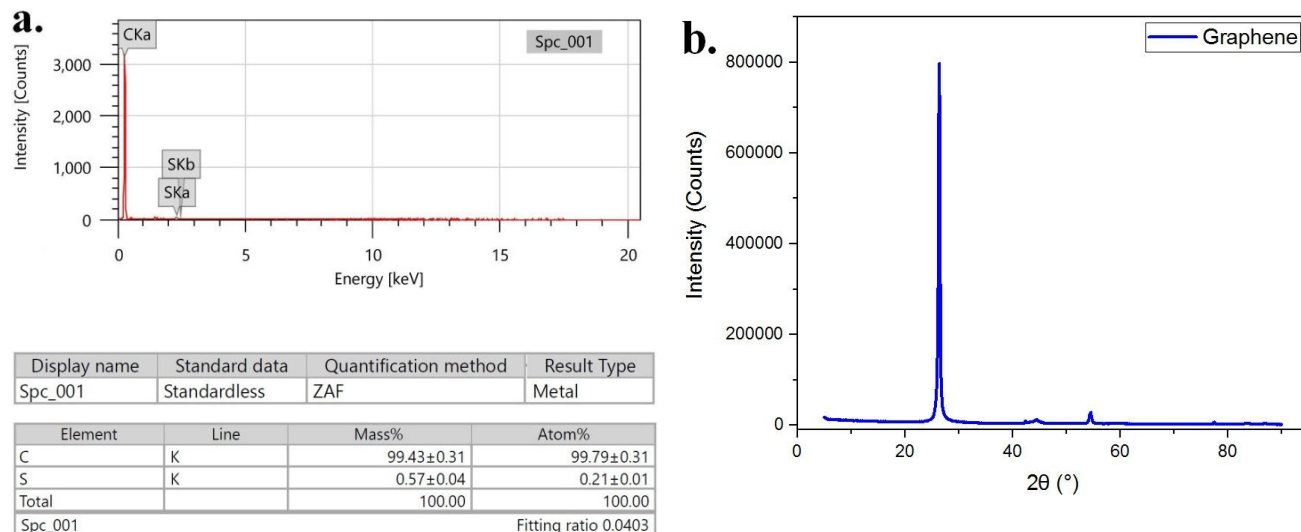


FIGURE 3. (a) Energy Dispersive X-ray (EDX) spectroscopy and (b) Analysis of powder X-ray Diffraction (XRD).

TABLE 2. Absorbance and comparative stability analysis of 30-minute and 60-minute ultrasonicated dielectric nanofluids over prolonged period of 90 days.

| DNFs → | 0.0015 wt% | | 0.003 wt% | | 0.006 wt% | | 0.01 wt% | |
|------------------------------|-------------------|--------|-----------|--------|-----------|--------|----------|--------|
| Ultrasonication time (min) → | 30 | 60 | 30 | 60 | 30 | 60 | 30 | 60 |
| Day ↓ | Absorbance (a.u.) | | | | | | | |
| Day 1 | 0.553 | 0.581 | 0.608 | 0.682 | 0.718 | 0.882 | 0.903 | 1.161 |
| Day 15 | 0.548 | 0.577 | 0.601 | 0.675 | 0.708 | 0.868 | 0.893 | 1.144 |
| Day 30 | 0.544 | 0.573 | 0.594 | 0.669 | 0.699 | 0.853 | 0.882 | 1.126 |
| Day 45 | 0.539 | 0.569 | 0.587 | 0.662 | 0.689 | 0.839 | 0.872 | 1.109 |
| Day 60 | 0.534 | 0.565 | 0.580 | 0.655 | 0.679 | 0.825 | 0.861 | 1.092 |
| Day 75 | 0.528 | 0.561 | 0.573 | 0.649 | 0.670 | 0.810 | 0.851 | 1.074 |
| Day 90 | 0.526 | 0.558 | 0.567 | 0.642 | 0.661 | 0.796 | 0.842 | 1.058 |
| Stability → (Day 90) | 95.17% | 96.13% | 93.21% | 94.16% | 92.04% | 93.11% | 90.22% | 91.13% |

0.01 wt%) and fixed ultrasonication time (30-minute and 60-minute) the absorbance reduces from day 1 to day 90. Thus, UV-Vis absorption can therefore be used to assess the long term stability of DNFs by comparing the long term absorption with the initial one. It is important to point out that day 90 stabilities of all DNFs presented in Table 2 were found to be more than 90%. Also, DNFs with 60-minute ultrasonicated time were more stable than those with 30-minute, indicating an improvement in the homogenous dispersion of nanoparticles inside DNFs.

The UV-Vis spectra for DNFs at all weight percentages and different ultrasonicated times are shown in Fig. 5 on day 30, 60, and 90. It is clear that the peak absorbance in all DNFs is located around the wavelength of 275 nm due to the presence of graphene particles. After this peak, all samples

exhibited a decrease in the absorbance. Also, it is evident from Fig. 5 that DNFs with 60-minute ultrasonication time were having higher absorbance at every measured wavelength as compared to the same DNFs with 30-minute ultrasonication time. This indicates that 60-minute ultrasonication time achieves more homogeneous dispersion and higher suspension stability of nanoparticles in DNFs.

VI. DIELECTRIC PROPERTIES OF NANOFUIDS AT LOW AND HIGH ULTRASONICATION PERIODS

This section presents comprehensive analysis for the dielectric properties of DNFs at low (30-minute) and high (60-minute) ultrasonication periods. The properties considered here include breakdown voltages at RTP under applied AC voltage and applied lightning impulse; and rel-

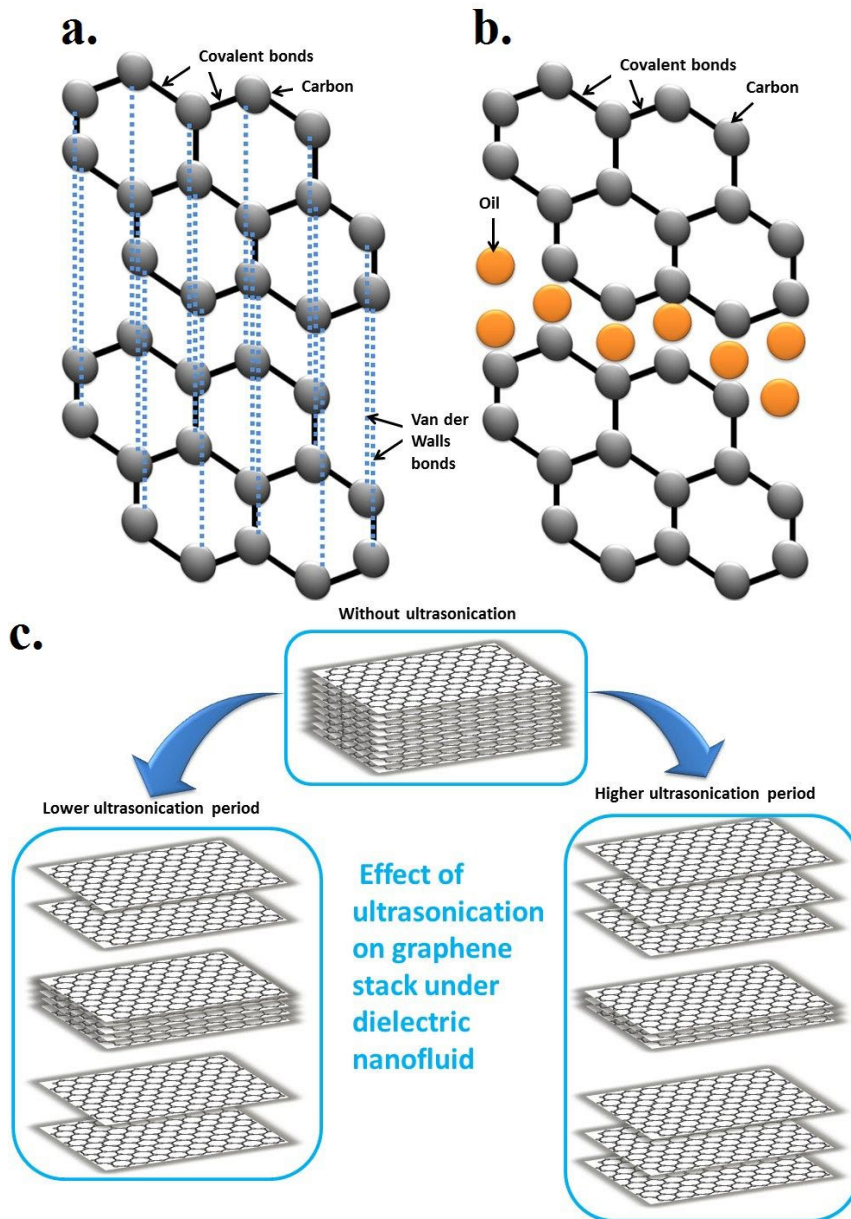


FIGURE 4. (a) Two layered graphene bound by Van der Waals bonds, (b) Two layered graphene with no Van der Waals bonds, and (c) Multilayered graphene stack in dielectric nanofluid (DNF) with no ultrasonication; lower ultrasonication time; and higher ultrasonication time.

ative permittivity, $\tan \delta$, and resistivity over a range of temperature from 45 °C to 90 °C.

A. AC BREAKDOWN VOLTAGE OF NANOFUIDS AT LOW AND HIGH ULTRASONICATION PERIODS

The dielectric breakdown voltage is a prime property of dielectric fluids, as it measures their ability to withstand electrical stress. This is the voltage at which the breakdown takes place between dual electrodes under predefined test conditions. In the current investigation AC BDV of DNFs were measured according to IEC 156. The mean value of AC breakdown voltage for the DBF was estimated to be 37.6 kV as presented in our previous investigation [19].

The inclusive mean AC breakdown voltage of DNFs for two ultrasonication periods (Viz., 30-minute and 60-minute) at varying graphene weight percentage (Viz., 0.0015 wt%, 0.003 wt%, 0.006 wt%, and 0.01 wt%) is presented in Table 3. It is evident that AC BDV was incremental in nature with the increase in the weight percentage of graphene either for 30-minute or 60-minute ultrasonicated DNFs. The highest mean AC BDV was measured as 51.6 kV and 53.2 kV at 0.01 wt% for 30-minute and 60-minute ultrasonicated samples, respectively. Percentage enhancements in mean AC BDV of all DNFs in comparison to DBF are also presented in Table 3. The highest percentage enhancement in mean AC BDV was measured as 37.23% and 41.49% at 0.01 wt%

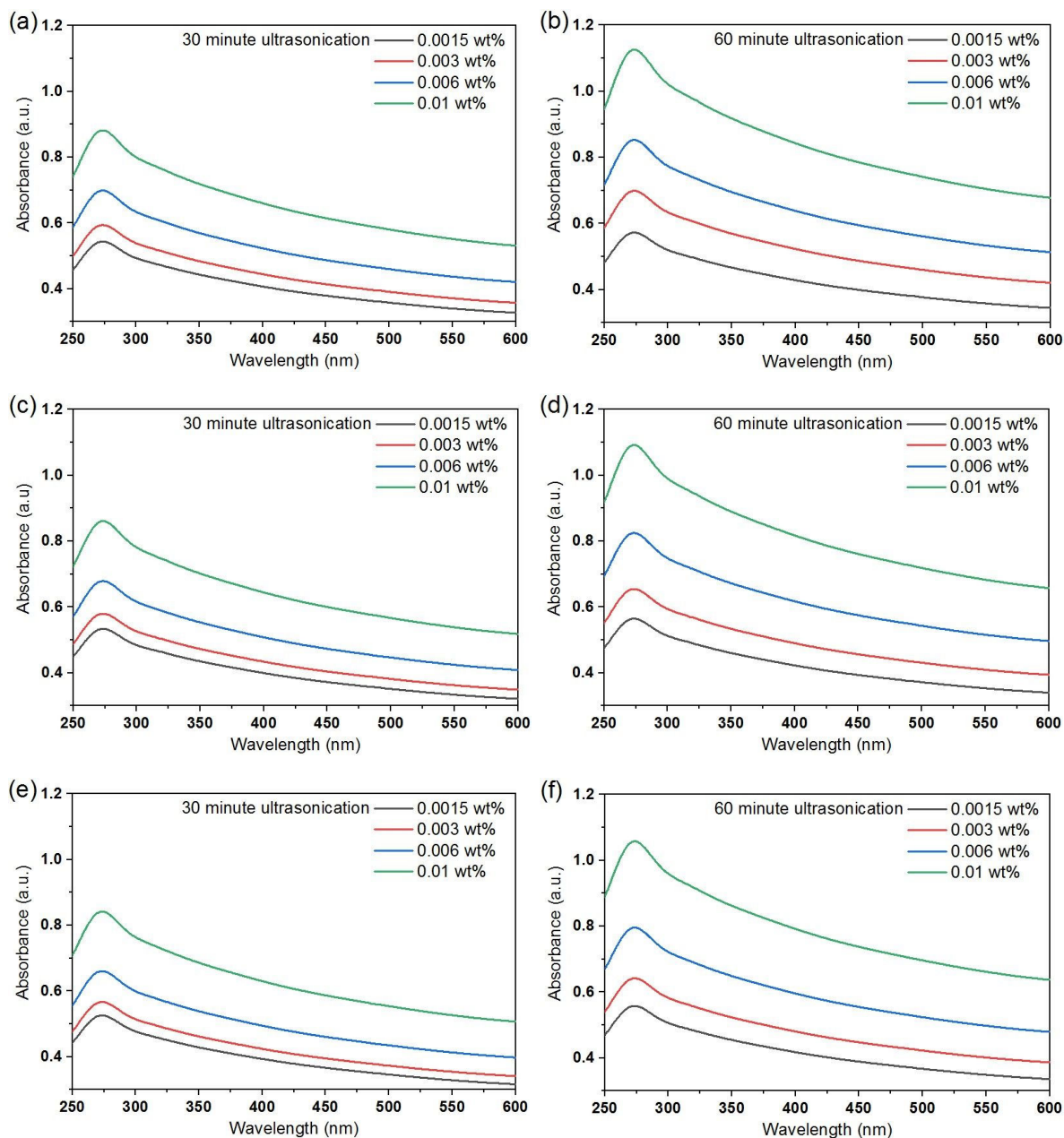


FIGURE 5. Absorbance of dielectric nanofluids with various filler levels and ultrasonicated times (Viz., 30-minute and 60-minute) on day: (a) and (b) 30; (c) and (d) 60; and (e) and (f) 90.

TABLE 3. Enhancement in AC breakdown voltages of dielectric nanofluids with ultrasonication time.

| DNFs → | 0.0015 wt% ↓ | | 0.003 wt% ↓ | | 0.006 wt% ↓ | | 0.01 wt% ↓ | |
|---|--------------|------|-------------|------|-------------|-------|------------|-------|
| Ultrasonication time (min.) | 30 | 60 | 30 | 60 | 30 | 60 | 30 | 60 |
| BDV (kV) | 38.1 | 38.4 | 39.2 | 39.8 | 44.9 | 45.6 | 51.6 | 53.2 |
| % Enh. (In comparison DBF) | 1.33 | 2.13 | 4.26 | 5.85 | 18.62 | 22.07 | 37.23 | 41.49 |
| % Enh. (In comparison 30 min. DNF) | - | 0.79 | - | 1.53 | - | 2.91 | - | 3.10 |

for 30-minute and 60-minute ultrasonicated samples, respectively. For all DNFs, 60-minute ultrasonicated DNFs recorded higher percentage enhancement of BDV in com-

parison to 30-minute ultrasonicated DNFs at fixed weight percentage of graphene. The percentage enhancement in BDV of 60-minute ultrasonicated DNFs in comparison to that

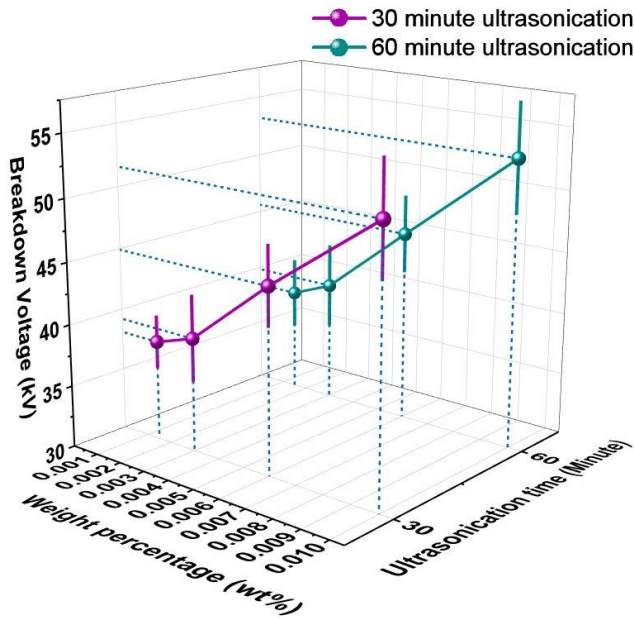


FIGURE 6. AC breakdown voltage of dielectric nanofluids with varying filler levels and ultrasonication time. Error bars represent standard deviation.

of 30-minute ultrasonicated DNFs is presented in Table 3. The percentage enhancements in BDV of 60-minute ultrasonicated DNFs were estimated as 0.79%, 1.53%, 2.91%, and 3.44% in comparison to that of 30-minute ultrasonicated DNFs at 0.0015 wt%, 0.003 wt%, 0.006 wt%, and 0.01 wt%, respectively. Fig. 6 shows AC breakdown voltage of DNFs with varying filler levels and ultrasonication time.

B. RELATIVE PERMITTIVITY OF NANOFLUIDS AT LOW AND HIGH ULTRASONICATION PERIODS

Relative permittivity is an AC characteristic, frequently denoted as dielectric constant. The relative permittivity of materials will influence the distribution of the local voltage stress. For oil-pressboard composite insulation system, more relative permittivity for the oil inherently leads to improved distribution of electrical stress along pressboard interface. In this section, relative permittivity of 30-minute and 60-minute ultrasonicated DNFs were compared at four varying temperatures.

As depicted in Fig. 7, relative permittivity of DNFs were plotted against weight percentages (Viz., 0.0015 wt%, 0.003 wt%, 0.006 wt%, and 0.01 wt%) for four sets of temperatures (Viz., 45°C, 60°C, 75°C and 90°C). It is evident that at a given weight percentage and temperature, 60-minute ultrasonicated DNFs had higher relative permittivity as compared to 30-minute ultrasonicated DNFs. Moreover, at a given weight percentage for both 30-minute and 60-minute ultrasonicated DNFs, highest relative permittivity was recorded at 45°C and decreased with the increase in the temperature up to 90°C. Furthermore, at 45°C, from 0.0015 wt% to 0.01 wt%, relative permittivity increased with the increase in weight

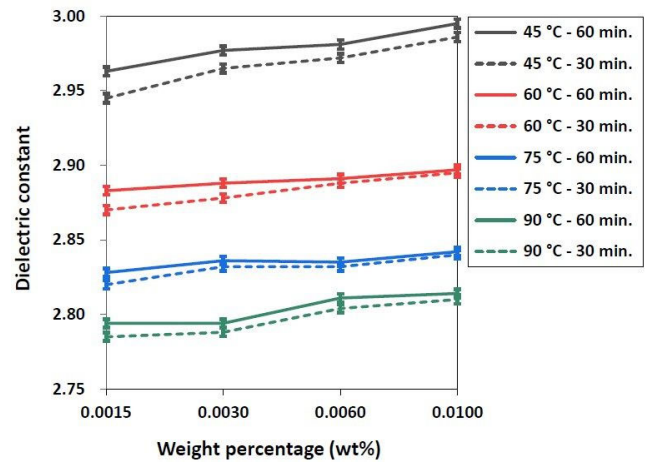


FIGURE 7. Relative permittivity of 60-minute and 30-minute ultrasonicated dielectric nanofluids at varying temperatures and fillers levels of graphene. Error bars represent experimental uncertainties.

percentage, for both 30-minute and 60-minute ultrasonicated DNFs.

The highest relative permittivity was observed at 0.01 wt% at 45°C, which was recorded as 2.995 for 60-minute ultrasonicated DNF against 2.986 for 30-minute ultrasonicated DNF. This consequently decreased the permittivity ratio of pressboard to oil and alleviated the non-uniformity of electric field distribution along pressboard interface. As displayed in Table 4, 60-minute ultrasonicated DNFs were compared to 30-minute ultrasonicated DNFs for relative permittivity. It is evident from Table 4, all DNFs with 60-minute ultrasonication time showed improved relative permittivity in comparison to same DNFs with 30-minute ultrasonication time. Although this improvement is small, but has an impact in improving electric field distribution along pressboard interface for 60-minute ultrasonicated DNFs compared to same DNFs with 30-minute ultrasonicated time.

C. TAN δ OF NANOFLUIDS AT LOW AND HIGH ULTRASONICATION PERIODS

Tan δ is the measurement of dielectric losses in liquid dielectrics that dissipate as heat energy when alternating electric field is applied. Inherently un-used natural esters yield higher tan δ compared to mineral oil, which was discussed in detail earlier [19], [20]. In this section, the effect of ultrasonication time on tan δ of DNFs are discussed in detail.

As shown in Fig. 8, tan δ of DNFs were plotted against weight percentages (Viz., 0.0015 wt%, 0.003 wt%, 0.006 wt%, and 0.01 wt%) for four sets of temperatures (Viz., 45°C, 60°C, 75°C and 90°C). It is obvious from Fig. 8, at a given weight percentage and temperature, 60-minute ultrasonicated DNFs were having lower tan δ as compared to 30-minute ultrasonicated DNFs. In addition, the lowest tan δ was recorded at 45°C at a given weight percentage for both 30-minute and 60-minute ultrasonicated DNFs and increased with a temperature increase up to 90°C. Moreover, at 45°C, from 0.0015 wt% to 0.01 wt%, tan δ decreased slightly with

TABLE 4. Property enhancement of 60-minute ultrasonicated dielectric nanofluids in comparison to 30-minute.

| wt% ↓ Property → | Property enhancement (%) ↓ | | | | | | | | | | | |
|---------------------|----------------------------|-------|-------|-------|-------|-------|-------|-------|-------------|------|------|------|
| | Relative permittivity | | | | Tan δ | | | | Resistivity | | | |
| | Temperature → | 45°C | 60°C | 75°C | 90°C | 45°C | 60°C | 75°C | 90°C | 45°C | 60°C | 75°C |
| 0.0015 wt% | 0.611 | 0.453 | 0.284 | 0.323 | -6.03 | -5.31 | -3.25 | -6.48 | 2.73 | 4.90 | 5.39 | 7.51 |
| 0.003 wt% | 0.405 | 0.347 | 0.141 | 0.215 | -7.91 | -6.01 | -3.69 | -4.12 | 4.08 | 3.78 | 5.32 | 7.79 |
| 0.006 wt% | 0.303 | 0.104 | 0.106 | 0.250 | -5.74 | -4.71 | -3.48 | -4.29 | 2.63 | 2.00 | 5.41 | 3.91 |
| 0.01 wt% | 0.301 | 0.069 | 0.070 | 0.142 | -3.91 | -4.48 | -0.47 | -1.79 | 2.46 | 2.78 | 3.77 | 5.29 |

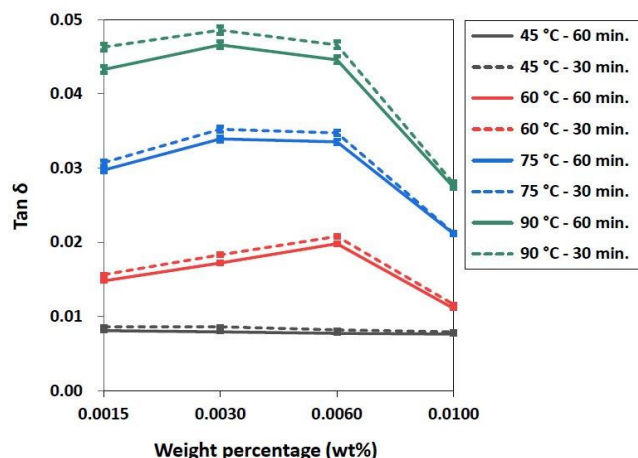


FIGURE 8. Tan δ of 60-minute and 30-minute ultrasonicated dielectric nanofluids at varying temperatures and fillers levels of graphene. Error bars represent experimental uncertainties.

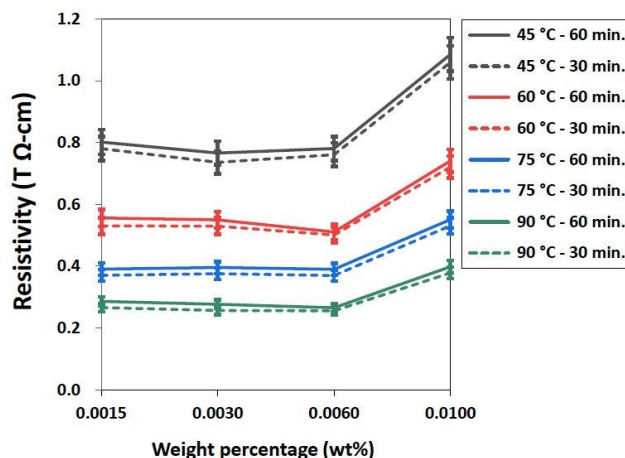


FIGURE 9. Resistivity of 60-minute and 30-minute ultrasonicated dielectric nanofluids at varying temperatures and fillers levels of graphene. Error bars represent experimental uncertainties.

the increase in weight percentage for both 30-minute and 60-minute ultrasonicated DNFs. For other temperatures, tan δ increased with the increase in weight percentage until a certain weight percentage, above which tan δ decreased.

The lowest tan δ was observed at 0.01 wt% at 45°C, recorded 0.00762 for 60-minute ultrasonicated DNF against 0.00793 for 30-minute ultrasonicated DNF. As shown in Table 4, 60-minute ultrasonicated DNFs were compared to 30-minute ultrasonicated DNFs for tan δ. Table 4 shows that all DNFs with 60-minute ultrasonication time showed lower tan δ compared to the same DNFs with 30-minute ultrasonication time. This decrement is substantial and will have a subsequent effect in reducing dielectric losses for 60-minute ultrasonicated DNFs compared to same DNFs with 30-minute ultrasonication time.

D. RESISTIVITY OF NANOFLUIDS AT LOW AND HIGH ULTRASONICATION PERIODS

A liquid’s volume resistivity is a direct-current calculation of the electrical insulating ability at opposite faces of a centimeter cube. The resistivity (Ω-cm) of a fluid is the ratio of the direct voltage gradient (V/cm) parallel to the current flow

within the fluid to the current density (A/cm²), at a specified time and under specified conditions.

As shown in Fig. 9, resistivity (T Ω-cm) of DNFs were plotted against weight percentages (Viz., 0.0015 wt%, 0.003 wt%, 0.006 wt%, and 0.01 wt%) for four sets of temperatures (Viz., 45°C, 60°C, 75°C and 90°C). It is obvious that at a given weight percentage and temperature, 60-minute ultrasonicated DNFs were having higher resistivity as compared to 30-minute ultrasonicated DNFs. Moreover, at a given weight percentage for both 30-minute and 60-minute ultrasonicated DNFs, highest resistivity was recorded at 45°C and decreased with the increase in the temperature up to 90°C. Furthermore, at 45°C, from 0.0015 wt% to 0.0060 wt%, resistivity slightly decreased with the increase in weight percentage, for both 30-minute and 60-minute ultrasonicated DNFs. Above 0.0060 wt%, resistivity increased with the increase in weight percentage, for both 30-minute and 60-minute ultrasonicated DNFs. Similar trend was observed at other temperatures.

The highest resistivity was observed at 45°C. At 0.0015 wt%, it was recorded 0.8013 T Ω-cm for 60-minute ultrasonicated DNF against 0.78 T Ω-cm for 30-minute ultrasonicated DNF. As shown in Table 4, 60-minute ultrasonicated DNFs were compared to 30-minute ultrasonicated

DNFs for resistivity. It is evident that all DNFs with 60-minute ultrasonication time showed improved resistivity in comparison to same DNFs with 30-minute ultrasonication time. This improvement is important for the performance of DNFs as an insulating medium.

VII. THERMAL CONDUCTIVITY OF NANOFLUIDS AT LOW AND HIGH ULTRASONICATION PERIODS

This section presents thermal properties of DNFs at high (60-minute) ultrasonication period compared to low (30-minute) ultrasonication period. Thermal properties include thermal conductivity over a temperature range from 35 °C to 65 °C and thermal response.

A. THERMAL CONDUCTIVITY OF NANOFLUIDS

Thermal conductivity and viscosity are the most important properties that indicate the cooling efficiency of the dielectric fluids used in transformers. In the current investigation it is assumed viscosity levels are within the specific typical

values because of lower weight percentage of graphene in the DNFs. On the other hand, it is important to provide specific typical values of the thermal conductivity for the optimization of thermal design. In this section thermal conductivity of 30-minute and 60-minute ultrasonicated DNFs were compared at four varying temperatures.

As depicted in Fig. 10 a-d, percentage enhancement in thermal conductivity of DNFs were plotted against temperatures (Viz., 35°C, 45°C, 55°C and 65°C), for four sets of weight percentages (Viz., 0.0015 wt%, 0.003 wt%, 0.006 wt%, and 0.01 wt%). It is obvious that at a given weight percentage and temperature, 60-minute ultrasonicated DNFs were having higher percentage enhancement in thermal conductivity as compared to 30-minute ultrasonicated DNFs. Moreover, at a given weight percentage for both 30-minute and 60-minute ultrasonicated DNFs, lowest percentage enhancement in thermal conductivity was recorded at 35°C and increased with the increase in the temperature up to 65°C.

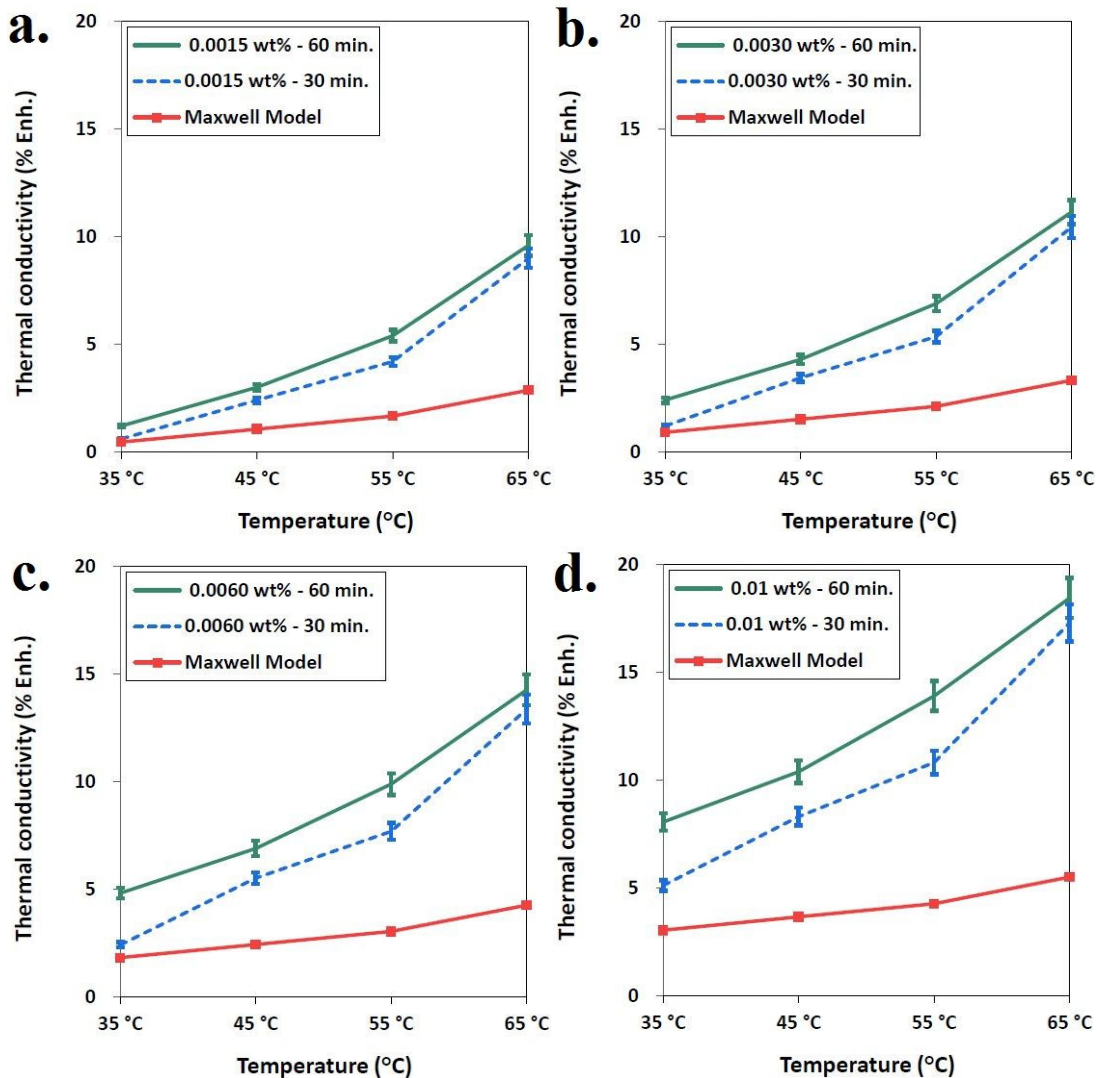


FIGURE 10. Percentage enhancement in thermal conductivity of 60-minute and 30-minute ultrasonicated dielectric nanofluids at varying temperatures and filler levels (a) 0.0015 wt%, (b) 0.0030 wt%, (c) 0.0060 wt%, and (d) 0.01 wt%. Error bars represent experimental uncertainties.

Furthermore, percentage enhancement in thermal conductivity increased with the increase in weight percentage of graphene.

The base value for finding a percentage increase in thermal conductivity is the thermal conductivity of DBF that obtained experimentally as 0.167 W/m.K at 35°C, 0.167 W/m.K at 45°C, 0.167 W/m.K at 55°C and 0.168 W/m.K at 65°C; was almost constant and compatible with that depicted in the literature [40]. Among all DNFs, the maximum enhancement in thermal conductivity was recorded 18.44% and was observed at 0.01 wt% and 65°C with 60-minute ultrasonication, while the same DNF with 30-minute ultrasonication exhibited an enhancement of 17.28%. In Fig. 10, percentage increase in thermal conductivity according to the Maxwell model is also plotted. Actual measured values of thermal conductivity results are significantly higher than the Maxwell model, which is the same as the results obtained by researchers [41]–[43].

B. THERMAL RESPONSE OF NANOFUIDS

Thermal response is another analysis to check the thermal effectiveness of 60-minute ultrasonicated DNFs for heat dissipation compared to 30-minute ultrasonicated DNFs. Custom-built thermal response test setup, as depicted in Fig. 11, was used to investigate the effectiveness of heating and cooling processes through digital thermometer. DC supply at a fixed power level was used to heat DNFs through micro coil for 26 minutes to investigate the effectiveness of heat dissipation, and then DNFs were allowed to cool down naturally for the next 26 minutes to investigate the effectiveness of cooling. To ensure the same conditions for all samples, the ambient temperature in the lab was maintained constant through air conditioner.

The thermal response test results are shown in Fig. 12(a), and (b) for the heating and cooling process, respectively. In Fig. 12(a), the temperature was recorded over different time intervals (i.e., minute 16, 18, 20, 22, 24, and 26) by the digital thermometer up to the initial 26 minutes. From the results, it is evident that at each weight percentage 60-minute ultrasonicated DNFs showed higher temperatures compared to 30-minute ultrasonicated DNFs, indicating more effectiveness in heat dissipation. On the other hand,

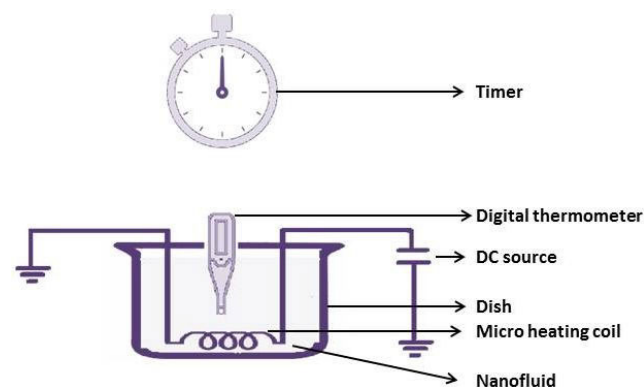


FIGURE 11. Custom-built thermal response test setup.

Fig. 12(b) shows the temperature for the next 26 minutes recorded at different time intervals (i.e., minute 42, 44, 46, 48, 50, and 52). From the results, it is evident that at each weight percentage 60-minute ultrasonicated DNFs showed lower temperatures compared to 30-minute ultrasonicated DNFs, indicating more cooling efficiency.

VIII. DISCUSSION

A. DIELECTRIC PERFORMANCE

In the composite fluids, the dielectric constant is directly proportional to the number of liquid molecules and the number of solid particles per unit volume. The number of liquid molecules per unit volume is independent of the ultrasonication period. But, the number of dispersed nanoparticle sheets per unit volume increases at a higher ultrasonication time compared to lower one, resulting in a small increase in relative permittivity. Fig. 13 shows schematic diagram showing mechanism for varying properties due to ultrasonication time. For DNFs with 30-minute ultrasonication time in Fig. 13(a), nanoparticles become less dispersive and exhibit some agglomerations causing fewer dispersed graphene nanoparticle sheets per unit volume. For DNFs with 60-minute ultrasonication time in Fig. 13(b), nanoparticles become more dispersive across the fluid causing more dispersed graphene nanoparticle sheets per unit volume. This results in increased relative permittivity compared to 30-minute ultrasonication DNF.

The better dispersion of nanoparticles for 60-minute ultrasonication DNF increases the number of dispersed nanoparticle sheets per unit volume. This creates more trapping sites across the fluid, either originated from nanoparticles themselves or originated from EDLs surrounding them. These trapping sites result in an increase in AC BDV compared to 30-minute ultrasonication DNF. Also, the increase in trapping sites with the better dispersion decreases the mobility of charge carriers with a subsequent increase in resistivity and decrease in $\tan \delta$.

B. THERMAL PERFORMANCE

The reason for the increase in thermal conductivity with the higher ultrasonication time is attributed to breaking up larger nanoparticle clusters and the detachment of individual graphene nanosheets. This increases the number of dispersed nanosheets per unit volume as shown in Fig. 13. Considering that thermal performance is governed by phonon transport, Brownian motion, and interparticle interactions due to EDL [20], the increased number of dispersed nanoparticle sheets contributes positively to all of these mechanisms. For phonon transport, the dispersion of graphene nanosheets increases the number of phonon polarization branches resulting in an increase in ballistic phonons with a consequent increase in heat transfer process. For Brownian motion and interparticle interactions, both thermal conductivity terms are directly proportional to the number of nanoparticles, making it beneficial to disperse graphene nanosheets with the

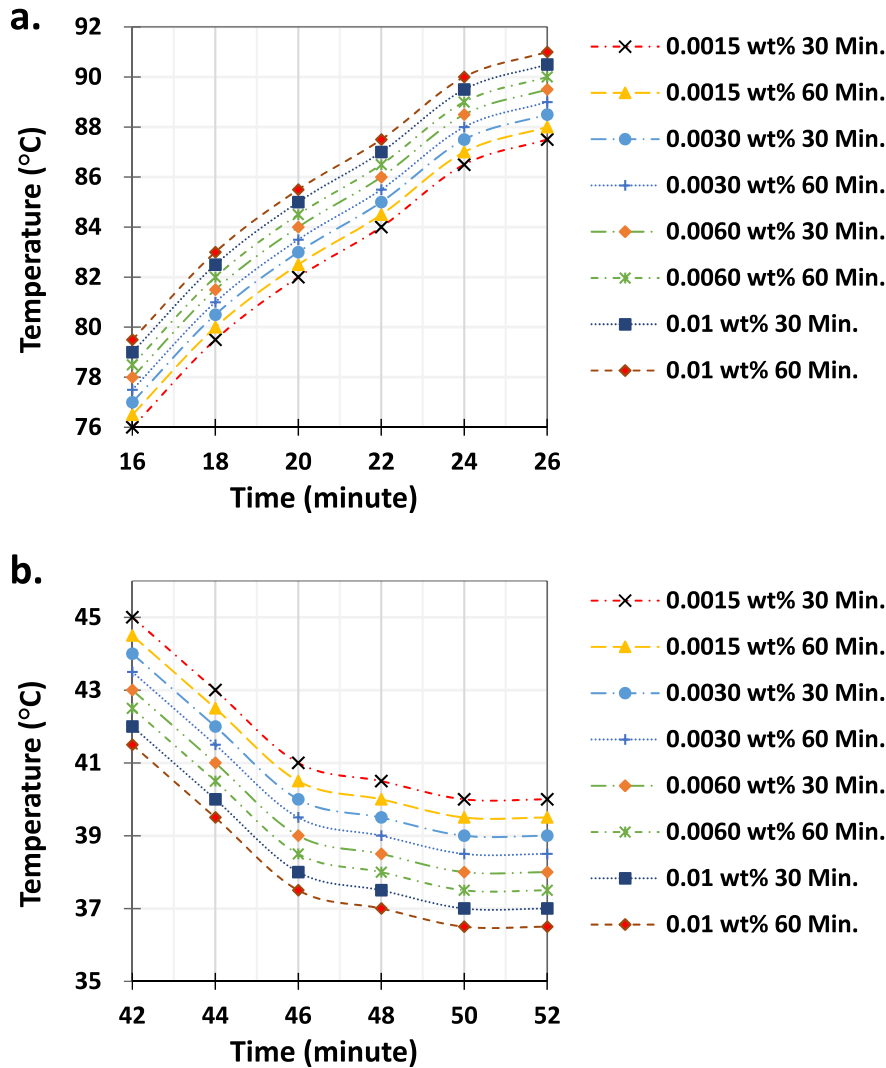


FIGURE 12. Thermal response of dielectric nanofluids: (a) Heating for the first 26 minutes, and (b) Natural cooling for the minute 27 to 52.

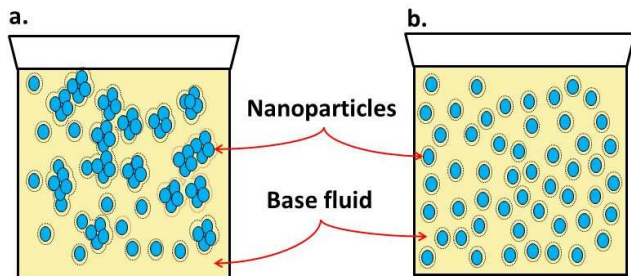


FIGURE 13. Schematic diagram showing mechanism for varying properties due to ultrasonication time: a) 30-minute ultrasonication time: less homogeneous and less dispersed nanoparticles per unit space, b) 60-minute ultrasonication time: more dispersed nanoparticles per unit space.

higher ultrasonication time. The obtained enhancements in all these mechanisms are also reflected on the thermal response, including heating and cooling processes. The thermal conductivity enhancements with temperature are attributed to

the positive impact of temperature on the abovementioned mechanisms. For phonon transport, the nanostructures vibrate in a faster way with increased temperature resulting in an increase in the number of phonons and subsequent increase in thermal conductivity enhancement. For Brownian motion and interparticle interactions, increased temperature results in an increase in Brownian motion [44] giving rise of thermal conductance.

IX. CONCLUSION

In the current research, long term stable cottonseed oil (CSO) based nanofluids were synthesized for the application as DNFs. Graphene nanoparticles were used at different weight fractions (0.0015 wt%, 0.003 wt%, 0.006 wt%, and 0.01 wt%) and nanofluids were prepared with different ultrasonication periods (10, 20, 30 and 60-minute). The graphene morphology and stacking were successfully characterized

using SEM, TEM, EDX, and XRD. For nanofluids, the prepared samples were kept stationary for a period of 2 week and thus were examined by visual inspection. It was found that the samples prepared with the ultrasonication period of 60-minute and 30-minute are more stable than others (10-minute and 20-minute). Thus, these periods were adopted for quantitative evaluation of stability through using UV-Vis spectroscopy, and for dielectric and thermal property measurements.

- DNFs with 60-minute ultrasonication time had higher absorbance and subsequent more homogenous dispersion and stable suspension of nanoparticles at every measured wavelength as compared to the same DNFs with 30-minute ultrasonication time. Based on relative concentration, stability after 90 days for 60-minute ultrasonicated samples was measured to be 96.13%, 94.16%, 93.11%, and 91.13%, where for 30-minute ultrasonicated samples it was 95.17%, 93.21%, 92.04%, and 90.22%, respectively at 0.0015 wt%, 0.003 wt%, 0.006 wt%, and 0.01 wt%. This was reflected positively on the dielectric and thermal properties.
- For the dielectric properties, the base value for finding a percentage enhancement in the AC BDV is the AC BDV of DBF, the percentage enhancements in AC BDV (at RTP) of 60-minute ultrasonicated DNFs were higher than that of 30-minute ultrasonicated DNFs at all weight fractions. The highest percentage enhancement in mean AC BDV was obtained at 0.01 wt% and was measured as 41.49% for 60-minute ultrasonicated sample, while for the same weight fraction it was measured as 37.23% for 30-minute ultrasonicated sample.
- Similarly, all DNFs with 60-minute ultrasonication period showed higher relative permittivity, lower $\tan \delta$, and higher resistivity compared to those with 30-minute ultrasonication period at given temperatures (i.e., 45°C, 60°C, 75°C and 90°C).
- For thermal properties, the base value for finding a percentage increase in the thermal conductivity is the thermal conductivity of DBF, the maximum enhancement in thermal conductivity was recorded 18.44% and was observed at 0.01 wt% and 65°C with 60-minute ultrasonication, while the same DNF at same temperature with 30-minute ultrasonication exhibited an enhancement of 17.28%. Similarly, thermal response test indicated all DNFs with 60-minute ultrasonication are more effective in heat dissipation and cooling.
- The results were explained considering the number of dispersed nanoparticle sheets per unit volume which increases at a higher ultrasonication time compared to lower one. This creates more trapping sites across the fluid, resulting in an increase in AC BDV and a decrease in the mobility of charge carriers with a subsequent increase in resistivity and decrease in $\tan \delta$. For thermal performance, the increased number of dispersed nanoparticle sheets contributed positively

towards phonon transport, Brownian motion, and inter-particle interactions due to EDL.

The presented results showed the relation between dispersion stability and thermo-dielectric properties. This contributes to the key issue of the long-term stability of the natural ester graphene nanofluids when working within a transformer.

REFERENCES

- [1] S. Singha, R. Asano, G. Frimpong, C. C. Claiborne, and D. Cherry, "Comparative aging characteristics between a high oleic natural ester dielectric liquid and mineral oil," *IEEE Trans. Dielectr. Electr. Insul.*, vol. 21, no. 1, pp. 149–158, Feb. 2014.
- [2] J. Tokunaga, H. Koide, K. Mogami, and T. Hikosaka, "Comparative studies on the aging of thermally upgraded paper insulation in palm fatty acid ester, mineral oil, and natural ester," *IEEE Trans. Dielectr. Electr. Insul.*, vol. 23, no. 1, pp. 258–265, Feb. 2016.
- [3] O. H. A. Fernandez, I. Fofana, J. Jalbert, S. Gagnon, E. Rodriguez-Celis, S. Duchesne, and M. Ryadi, "Aging characterization of electrical insulation papers impregnated with synthetic ester and mineral oil: Correlations between mechanical properties, depolymerization and some chemical markers," *IEEE Trans. Dielectr. Electr. Insul.*, vol. 25, no. 1, pp. 217–227, Feb. 2018.
- [4] L. Loïselle, U. Rao, and I. Fofana, "Influence of aging on oil degradation and gassing tendency for mineral oil and synthetic ester under low energy discharge electrical faults," *Energies*, vol. 13, no. 3, Jan. 2020, Art. no. 595.
- [5] B. Garcia, T. Garcia, V. Primo, J. C. Burgos, and D. Urquiza, "Studying the loss of life of natural-ester-filled transformer insulation: Impact of moisture on the aging rate of paper," *IEEE Electr. Insul. Mag.*, vol. 33, no. 1, pp. 15–23, Jan. 2017.
- [6] M. M. M. Salama, D.-E.-A. Mansour, M. Daghrah, S. M. Abdelkasoud, and A. A. Abbas, "Thermal performance of transformers filled with environmentally friendly oils under various loading conditions," *Int. J. Electr. Power Energy Syst.*, vol. 118, Jun. 2020, Art. no. 105743.
- [7] M. Rafiq, M. Shafique, A. Azam, and M. Ateq, "The impacts of nanotechnology on the improvement of liquid insulation of transformers: Emerging trends and challenges," *J. Mol. Liquids*, vol. 302, Mar. 2020, Art. no. 112482.
- [8] N. A. Azizie and N. Hussin, "Preparation of vegetable oil-based nanofluid and studies on its insulating property: A review," *J. Phys., Conf. Ser.*, vol. 1432, Jan. 2020, Art. no. 012025.
- [9] J. Jacob, P. Preetha, and S. T. Krishnan, "Review on natural ester and nanofluids as an environmental friendly alternative to transformer mineral oil," *IET Nanodielectr.*, vol. 3, no. 2, pp. 33–43, Jun. 2020.
- [10] U. Khaled and A. Beroual, "Statistical investigation of AC dielectric strength of natural ester oil-based Fe₃O₄, Al₂O₃, and SiO₂ nano-fluids," *IEEE Access*, vol. 7, pp. 60594–60601, 2019.
- [11] R. Madavan, S. S. Kumar, and M. W. Iruthiyarajan, "A comparative investigation on effects of nanoparticles on characteristics of natural esters-based nanofluids," *Colloids Surf. A, Physicochem. Eng. Aspects*, vol. 556, pp. 30–36, Nov. 2018.
- [12] I. Fernández, R. Valiente, F. Ortiz, C. J. Renedo, and A. Ortiz, "Effect of TiO₂ and ZnO nanoparticles on the performance of dielectric nanofluids based on vegetable esters during their aging," *Nanomaterials*, vol. 10, no. 4, p. 692, Apr. 2020.
- [13] M. Makmud, H. Illias, C. Chee, and M. Sarjadi, "Influence of conductive and semi-conductive nanoparticles on the dielectric response of natural ester-based nanofluid insulation," *Energies*, vol. 11, no. 2, Feb. 2018, Art. no. 333.
- [14] K. N. Koutras, I. A. Naxakis, A. E. Antonelou, V. P. Charalampakos, E. C. Pyrgioti, and S. N. Yannopoulos, "Dielectric strength and stability of natural ester oil based TiO₂ nanofluids," *J. Mol. Liquids*, vol. 316, Oct. 2020, Art. no. 113901.
- [15] C. Olmo, C. Méndez, F. Ortiz, F. Delgado, and A. Ortiz, "Titania nanofluids based on natural ester: Cooling and insulation properties assessment," *Nanomaterials*, vol. 10, no. 4, Mar. 2020, Art. no. 603.
- [16] P. Thomas, N. E. Hudedmani, R. T. A. R. Prasath, N. K. Roy, and S. N. Mahato, "Synthetic ester oil based high permittivity CaCu₃Ti₄O₁₂ (CCTO) nanofluids an alternative insulating medium for power transformer," *IEEE Trans. Dielectr. Electr. Insul.*, vol. 26, no. 1, pp. 314–321, Feb. 2019.

- [17] J. Taha-Tijerina, H. Ribeiro, K. Aviña, J. M. Martínez, A. P. Godoy, J. M. D. O. Cremonuzzi, M. A. Luciano, M. A. G. Benega, R. J. E. Andrade, G. J. M. Fachine, G. Babu, and S. Castro, "Thermal conductivity performance of 2D h-BN/MoS₂-hybrid nanostructures used on natural and synthetic esters," *Nanomaterials*, vol. 10, no. 6, Jun. 2020, Art. no. 1160.
- [18] A. Beroual, H. B. H. Sitorus, R. Setiabudy, and S. Bismo, "Comparative study of AC and DC breakdown voltages in jatropha methyl ester oil, mineral oil, and their mixtures," *IEEE Trans. Dielectr. Electr. Insul.*, vol. 25, no. 5, pp. 1831–1836, Oct. 2018.
- [19] R. A. Farade, N. I. B. A. Wahab, D.-E.-A. Mansour, N. B. Azis, J. Jasni, N. R. Banapurmath, and M. E. M. Soudagar, "Investigation of the dielectric and thermal properties of non-edible cottonseed oil by infusing h-BN nanoparticles," *IEEE Access*, vol. 8, pp. 76204–76217, 2020.
- [20] R. A. Farade, N. I. A. Wahab, D.-E.-A. Mansour, N. B. Azis, J. B. Jasni, M. E. M. Soudagar, and V. Siddappa, "Development of graphene oxide-based nonedible cottonseed nanofluids for power transformers," *Materials*, vol. 13, no. 11, Jun. 2020, Art. no. 2569.
- [21] A. J. Worthen, V. Tran, K. A. Cornell, T. M. Truskett, and K. P. Johnston, "Steric stabilization of nanoparticles with grafted low molecular weight ligands in highly concentrated brines including divalent ions," *Soft Matter*, vol. 12, no. 7, pp. 2025–2039, 2016.
- [22] G. Dombek, Z. Nadolny, and P. Przybyłek, "The study of thermal properties of mineral oil and synthetic ester modified by nanoparticles TiO₂ and C₆₀," in *Proc. Int. Conf. High Voltage Eng. Appl. (ICHVE)*, Poznań, Poland, Sep. 2014, pp. 1–4.
- [23] M. V. Avdeev, M. Balasoiu, V. L. Aksenov, V. M. Garamus, J. Kohlbrecher, D. Bica, and L. Vekas, "On the magnetic structure of magnetite/oleic acid/benzene ferrofluids by small-angle neutron scattering," *J. Magn. Magn. Mater.*, vol. 270, no. 3, pp. 371–379, Apr. 2004.
- [24] L. Pislaru-Danescu, A. M. Morega, G. Telipan, M. Morega, J. B. Dumitru, and V. Marinescu, "Magnetic nanofluid applications in electrical engineering," *IEEE Trans. Magn.*, vol. 49, no. 11, pp. 5489–5497, Nov. 2013.
- [25] R. Liu, L. A. A. Pettersson, T. Auletta, and O. Hjortstam, "Fundamental research on the application of nano dielectrics to transformers," in *Proc. Annu. Rep. Conf. Electr. Insul. Dielectr. Phenomena*, Cancún, Mexico, Oct. 2011, pp. 423–427.
- [26] G. Shukla and H. Aiyer, "Thermal conductivity enhancement of transformer oil using functionalized nanodiamonds," *IEEE Trans. Dielectr. Electr. Insul.*, vol. 22, no. 4, pp. 2185–2190, Aug. 2015.
- [27] M. Rafiq, M. Shafique, A. Azam, and M. Ateeq, "Transformer oil-based nanofluid: The application of nanomaterials on thermal, electrical and physicochemical properties of liquid insulation—A review," *Ain Shams Eng. J.*, vol. 12, no. 1, pp. 555–576, Mar. 2021.
- [28] M. Gupta, V. Singh, S. Kumar, S. Kumar, N. Dilbaghi, and Z. Said, "Up to date review on the synthesis and thermophysical properties of hybrid nanofluids," *J. Cleaner Prod.*, vol. 190, pp. 169–192, Jul. 2018.
- [29] M. Rajnak, M. Timko, J. Kurimsky, B. Dolnik, R. Cimbala, T. Tobias, K. Paulovicova, J. F. M. L. Mariano, and P. Kopcansky, "Electrical conduction in a transformer oil-based magnetic nanofluid under a DC electric field," *J. Magn. Magn. Mater.*, vol. 459, pp. 191–196, Aug. 2018.
- [30] K. Zhang, L. Mao, L. L. Zhang, H. S. O. Chan, X. S. Zhao, and J. Wu, "Surfactant-intercalated, chemically reduced graphene oxide for high performance supercapacitor electrodes," *J. Mater. Chem.*, vol. 21, no. 20, pp. 7302–7307, 2011.
- [31] S. S. Sukumaran, K. B. Jinesh, and K. G. Gopchandran, "Liquid phase exfoliated graphene for electronic applications," *Mater. Res. Exp.*, vol. 4, no. 9, Sep. 2017, Art. no. 095017.
- [32] W. S. Sarsam, A. Amiri, S. N. Kazi, and A. Badarudin, "Stability and thermophysical properties of non-covalently functionalized graphene nanoplatelets nanofluids," *Energy Convers. Manage.*, vol. 116, pp. 101–111, May 2016.
- [33] F. Yu, Y. Chen, X. Liang, J. Xu, C. Lee, Q. Liang, P. Tao, and T. Deng, "Dispersion stability of thermal nanofluids," *Prog. Natural Sci., Mater. Int.*, vol. 27, no. 5, pp. 531–542, 2017.
- [34] X. Wang and L. Zhang, "Green and facile production of high-quality graphene from graphite by the combination of hydroxyl radicals and electrical exfoliation in different electrolyte systems," *RSC Adv.*, vol. 9, no. 7, pp. 3693–3703, 2019.
- [35] Y.-J. Wan, L.-C. Tang, D. Yan, L. Zhao, Y.-B. Li, L.-B. Wu, J.-X. Jiang, and G.-Q. Lai, "Improved dispersion and interface in the graphene/epoxy composites via a facile surfactant-assisted process," *Compos. Sci. Technol.*, vol. 82, pp. 60–68, Jun. 2013.
- [36] A. Asadi, F. Pourfattah, I. M. Szilágyi, M. Afrand, G. Żyła, H. S. Ahn, S. Wongwises, H. M. Nguyen, A. Arabkoohsar, and O. Mahian, "Effect of sonication characteristics on stability, thermophysical properties, and heat transfer of nanofluids: A comprehensive review," *Ultrason. Sonochem.*, vol. 58, Nov. 2019, Art. no. 104701.
- [37] M. Mehrali, E. Sadeghinezhad, S. Latibari, S. Kazi, M. Mehrali, M. N. B. M. Zubir, and H. S. Metselaar, "Investigation of thermal conductivity and rheological properties of nanofluids containing graphene nanoplatelets," *Nanos. Res. Lett.*, vol. 9, no. 1, 2014, Art. no. 15.
- [38] Z. Chen, A. Shahsavari, A. A. A. Al-Rashed, and M. Afrand, "The impact of sonication and stirring durations on the thermal conductivity of alumina-liquid paraffin nanofluid: An experimental assessment," *Powder Technol.*, vol. 360, pp. 1134–1142, Jan. 2020.
- [39] Z. Li, R. Kalbasi, Q. Nguyen, and M. Afrand, "Effects of sonication duration and nanoparticles concentration on thermal conductivity of silica-ethylene glycol nanofluid under different temperatures: An experimental study," *Powder Technol.*, vol. 367, pp. 464–473, May 2020.
- [40] E. E. G. Rojas, J. S. R. Coimbra, and J. Telis-Romero, "Thermophysical properties of cotton, canola, sunflower and soybean oils as a function of temperature," *Int. J. Food Properties*, vol. 16, no. 7, pp. 1620–1629, Oct. 2013.
- [41] W. Yu, H. Xie, L. Chen, and Y. Li, "Investigation of thermal conductivity and viscosity of ethylene glycol based ZnO nanofluid," *Thermochim. Acta*, vol. 491, nos. 1–2, pp. 92–96, Jul. 2009.
- [42] M. I. Pryazhnikov, A. V. Minakov, V. Y. Rudyak, and D. V. Guzei, "Thermal conductivity measurements of nanofluids," *Int. J. Heat Mass Transf.*, vol. 104, pp. 1275–1282, Jan. 2017.
- [43] A. Hemmati-Sarapardeh, A. Varamesh, M. N. Amar, M. M. Husein, and M. Dong, "On the evaluation of thermal conductivity of nanofluids using advanced intelligent models," *Int. Commun. Heat Mass Transf.*, vol. 118, Nov. 2020, Art. no. 104825.
- [44] J.-M. Liu, Z.-H. Liu, and Y.-J. Chen, "Experiment and calculation of the thermal conductivity of nanofluid under electric field," *Int. J. Heat Mass Transf.*, vol. 107, pp. 6–12, Apr. 2017.



RIZWAN A. FARADE received the B.E. degree in electrical and electronics engineering from Visvesvaraya Technological University, Belgaum, India, in 2005, and the M.Tech. degree in power electronics from Jawaharlal Nehru Technological University, Hyderabad, India, in 2013. He is currently pursuing the Ph.D. degree in electrical and electronics engineering with University Putra Malaysia, Serdang, Malaysia. Since 2009, he has been a Lecturer and an Assistant Professor in

India's diploma and undergraduate programs. Since 2014, he has been with Kalsekar Technical Campus, New Mumbai, India, as an Assistant Professor in undergraduate program. His research interests include dielectric fluids, power systems, and nano biodiesel.



NOOR IZZRI ABDUL WAHAB (Senior Member, IEEE) received the degree in electrical and electronic engineering from the University of Manchester Institute of Science and Technology (UMIST), U.K., in 1998, the M.Sc. degree in electrical power engineering from Universiti Putra Malaysia (UPM), in 2002, and the Ph.D. degree in electrical, electronic and system engineering from Universiti Kebangsaan Malaysia (UKM), in 2010. He is currently an Associate Professor with the

Department of Electrical and Electronic Engineering, Faculty of Engineering, UPM. He is also the Founding Member of the Advanced Lighting, Power and Energy Research Centre (ALPER), UPM. His research interests include power system stability, application of AI in power systems, and power quality. He is a registered Chartered Engineer (C.Eng.), a Professional Engineer (Ir.), and a member of The Institution of Engineers Malaysia (IEM).



DIAA-ELDIN A. MANSOUR (Senior Member, IEEE) was born in Tanta, Egypt, in December 1978. He received the B.Sc. and M.Sc. degrees in electrical engineering from Tanta University, Tanta, in 2000 and 2004, respectively, and the Ph.D. degree in electrical engineering from Nagoya University, Nagoya, Japan, in 2010. Since 2000, he has been with the Department of Electrical Power and Machines Engineering, Faculty of Engineering, Tanta University, working as an Instructor, an Assistant Lecturer, and currently, a Professor and the Director of the High Voltage and Superconductivity Laboratory. In 2010, he was a Foreign Researcher for three months at the EcoTopia Science Institute, Nagoya University. His research interests include high-voltage engineering, condition monitoring and diagnosis of electrical power equipment, nanodielectrics, and applied superconductivity. He received the Best Presentation Award two times from IEE of Japan in 2008 and 2009, the Prof. Khalifa's Prize from the Egyptian Academy of Scientific Research and Technology in 2013, the Tanta University Encouragement Award in 2017, and the State Encouragement Award in 2018.



NORHAFIZ B. AZIS (Senior Member, IEEE) received the B.Eng. degree in electrical and electronic engineering from Universiti Putra Malaysia, Malaysia, in 2007, and the Ph.D. degree in electrical power engineering from The University of Manchester, U.K., in 2012. He is currently an Associate Professor with the Department of Electrical and Electronic Engineering, Universiti Putra Malaysia. His research interests include in-service ageing of transformer insulation, condition monitoring, asset management, and alternative insulation materials for transformers.



JASRONITA BT. JASNI (Senior Member, IEEE) received the B.Eng. and M.Eng. degrees in electrical engineering from Universiti Teknologi Malaysia, Johor, Malaysia, in 1998 and 2001, respectively, and the Ph.D. degree in electrical power engineering from Universiti Putra Malaysia, Selangor, Malaysia, in 2010. From 1998 to 1999, she was a System Engineer and later from 1999 to 2001, she has worked as a Tutor with the Department of Electrical and Electronics Engineering, Faculty of Engineering, Universiti Putra Malaysia, where she started working as a Lecturer in 2001. She is currently an Associate Professor with the Department of Electrical and Electronics Engineering, Faculty of Engineering, Universiti Putra Malaysia. Her research interests include power systems, renewable energy, and lightning protection. She has received several awards and recognitions for her work and researches, including the Excellent in Service Award (Universiti Putra Malaysia), the Excellent in Teaching Award (Universiti Putra Malaysia), and the Bronze Medal in Malaysia Technology Expo.



VEERAPANDIYAN VEERASAMY (Graduate Student Member, IEEE) received the bachelor's degree in electrical and electronics engineering from the Panimalar Engineering College, India, in 2013, and the M.E. degree in power systems engineering from the Government College of Technology, India, in 2015. He is currently pursuing the Ph.D. degree in power systems with Universiti Putra Malaysia, Malaysia. Since 2015, he has been working as an Assistant Professor with the Department of Electrical and Electronics Engineering, Rajalakshmi Engineering College, India. His research interests include the design of robust controllers for power system application, fault classification, and power system monitoring.



MARIAMMAL THIRUMENI received the B.E. degree in electrical and electronics engineering from Manonmaniam Sundaranar University, Tirunelveli, the master's degree in engineering from the College of Engineering, Guindy, and the Ph.D. degree from VIT University, Chennai. She is currently working as an Assistant Professor (SG) with the Rajalakshmi Engineering College. Her research interests include control systems, power electronics, power systems, and intelligent controllers.



ANDREW XAVIER RAJ IRUDAYARAJ (Graduate Student Member, IEEE) received the bachelor's degree in electrical and electronics engineering from the J. J. College of Engineering and Technology, Trichy, India, in 2012, and the M.E. degree in control and instrumentation engineering from the SRM Valliammai Engineering College, Chennai, India, in 2014. He is currently pursuing the Ph.D. degree in power systems with UPM, Malaysia. Since 2014, he has been working as an Assistant Professor with the Department of Electronics and Instrumentation Engineering, SRM Valliammai Engineering College. His research interests include the design of robust controllers for power system applications, system modeling, nonlinear controllers, and stability studies.



AVINASH SRIKANTA MURTHY received the B.Eng. degree in electrical and electronics engineering from the Malnad College of Engineering, in 2011, and the M.Tech. degree in power and energy systems from the National Institute of Technology Karnataka, Surathkal, in 2013. He is currently pursuing the Ph.D. degree in advanced lightning, power and energy research (ALPER) with the Department of Electrical and Electronics Engineering, Faculty of Engineering, Universiti Putra Malaysia. He has been working with Rural Electrification Corporation under the Ministry of Power, India, as a Lead Electrical Engineer, until 2015. His research interests include transformers, power cables, and computational electromagnetics.

...